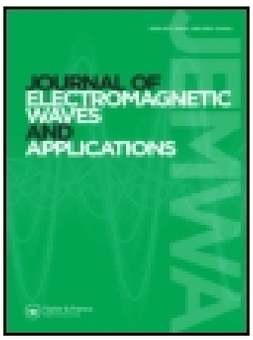

Journal of Electromagnetic Waves and Applications

ISSN: (Print) (Online) Journal homepage: https://www.tandfonline.com/loi/tewa20

Element excitation optimization for phased array fault diagnosis

K. P. Prajosh , Uday K. Khankhoje & Francesco Ferranti

To cite this article: K. P. Prajosh , Uday K. Khankhoje & Francesco Ferranti (2020): Element excitation optimization for phased array fault diagnosis, Journal of Electromagnetic Waves and Applications

To link to this article: https://doi.org/10.1080/09205071.2020.1825123

Published online: 29 Sep 2020.

JOURNAL OF ELECTROMAGNETIC WAVES AND APPLICATIONS
https://doi.org/10.1080/09205071.2020.1825123

Taylor & Francis
Taylor & Francis Group

Element excitation optimization for phased array fault diagnosis

K. P. Prajosh [a], Uday K. Khankhoje [a] and Francesco Ferranti [b]

[a]Department of Electrical Engineering, Indian Institute of Technology Madras, Chennai, India; [b]Institut Mines-Télécom Atlantique, CNRS UMR 6285 Lab-STICC, Brest, France

ABSTRACT

We present techniques for solving the problem of detecting element failures in phased array antennas by using a combination of a single fixed probe and an optimization of element excitations using principles derived from compressive sensing. This departs significantly from conventional techniques where the excitations are held constant and probes are instead moved spatially to collect measurements. Doing so helps us to accomplish two objectives with regards to successful fault diagnosis. First, we achieve a reduction in the number of measurements required compared to the state of the art; this reduction is particularly significant in the case of high-noise measurements where existing methods fail. Second, our techniques solve the problem of fault diagnosis in the case of real valued measurements (i.e. intensity measurement along with phase detection instead of phase measurement), which leads to simpler measurement hardware. We use nonconvex optimization algorithms to generate numerical results in support of our conclusions.

ARTICLE HISTORY
Received 28 June 2020
Accepted 14 September 2020

KEYWORDS
Compressive sensing; antenna arrays; fault diagnosis

1. Introduction

Phased array antennas are widely used in wireless communications, remote sensing, and radar applications [1]. Future deployments of telecommunications [2] and automotive radars [3] will extensively rely on the proper functioning of such systems. The failure of one or more antenna elements can severely impair the system operation, making the monitoring of the health of these systems increasingly critical. In particular, methods of fault diagnosis that can work *in situ* with minimal modification are particularly appealing, rather than those that require systems to be taken inside specialized test facilities. For instance, recent work in wireless monitoring applications have used embedded antennas [4], where the antenna's proper functioning is to be assured for optimal operation.

In this article, we propose techniques of fault diagnosis that rely on a single fixed probe, and can work with complex or real valued measurement data in the near and far-field. Since we do not require probes to scan the array under test (AUT) from different spatial locations, the techniques are in-principle compatible with *in situ* measurements of the AUT in

CONTACT Uday K. Khankhoje uday@ee.iitm.ac.in

operational settings, provided that scattering from the neighboring environment can be minimized.

The typical use-case scenario for fault diagnosis considered in recent literature has centered around element failure of a *small* fraction of the total element number. In this scenario, the principles of compressive sensing (CS) [5] have offered the promise of fault diagnosis by making much fewer measurements than the number of antennas in the array [6]. Several variations on this theme have been studied, such as fault diagnosis from near [6] or far [7] field data, and from measurements with [8] and without [9] phase. It is known that for CS techniques to work, the sensing matrix must satisfy the so-called "Restrictive Isometry Property" (RIP) [10]. A matrix A of size $n \times m$ ($n < m$) is said to satisfy the $s-$RIP with a constant δ_s if the following relation holds true for any sub-matrix A_s formed by choosing s ($< n$) columns of A:

$$(1 - \delta_s)\|x\|_2^2 \leq \|A_s x\|_2^2 \leq (1 + \delta_s)\|x\|_2^2, \quad \forall\, x \in \mathbb{R}^s. \tag{1}$$

By choosing the measurement locations in a particular way [7], it was shown that the sensing matrix was a random partial Fourier matrix, which in turn satisfied RIP provided sufficient measurements were made.

Typically, the RIP property is difficult to verify in practise, and often the CS machinery is used in a heuristic manner by resorting to random measurement locations [9]. Instead of the RIP, it is known that minimizing the mutual coherence of the sensing matrix provides (weaker) guarantees of convergence [11]; recent work has shown how this idea can be applied to electromagnetic compressive sensing applications [12]. Returning to the theme of fault diagnosis in phased arrays, we note that in all the work referred to so far, the sensing matrix was generated by choosing different sensing locations in space. This imposes severe restrictions on how suitable the sensing matrices are for applying CS principles.

Recent work [13,14] has shown an elegant method of fault diagnosis where the probe locations are kept fixed and the phase of the element excitations are varied to generate a series of measurements. The phases were chosen at random and fault diagnosis was accomplished by solving an unconstrained ℓ_p minimization problem ($0 < p \leq 1$). We extend this idea further by allowing the *entire* sensing matrix to be subject to design. In particular, we allow both the amplitude and phases of the element excitations to be optimized in order to minimize the mutual coherence of the sensing matrix. The theory of compressive sensing tells us that by doing so, the number of measurements required for successful fault diagnosis can be reduced, much more so in the average case as compared to the worst case [15, Ch. 7].

In our work we consider two types of measurements, depending on the type of hardware available. We denote the phasor of a time-harmonic electromagnetic field by $re^{j\theta}$, where r and θ represent the amplitude and phase, respectively. Then, the measurements are defined as follows:

- A *complex* measurement is one which measures both the amplitude (r) and the phase (θ) via measurements of the in-phase and quadrature components.
- A *real* measurement is one which measures the amplitude (r) and the sign of the in-phase component ($\mathrm{sgn}(\cos\theta)$); this can be implemented by using a power meter (measurement $\propto r^2$) and a phase detector to determine the sign given a known reference.

Since the latter type of measurement does not actually *measure* the phase, a real measurement requires simpler hardware than a complex measurement and offers the possibility of cheaper hardware for large scale Internet of Things (IoT) type of applications.

In our approach, the same technique can be used for solving *both* problems without any approximations, and the only difference lies in the nature of the sensing matrix that is employed. This is accomplished in the real measurements case by a specific choice of the element excitation phase which will be detailed subsequently. This confers a great deal of generality to our approach, not previously offered by other approaches. We note that there exists a related problem of fault diagnosis using intensity-only (or phase-less) measurements (e.g. [9]); however, we do not address this problem in the current work.

This paper is organized as follows: we formulate the problem mathematically in Section 2, where we also describe the solution strategies. In Section 3, we present numerical results in support of the efficacy of our technique for complex and real measurements along with their analysis. Finally, we conclude in Section 4 with a summary of our results.

2. Problem formulation and methods

2.1. Problem setup

We consider the measured far-field, $E(\theta)$, from a one dimensional N-element array of elements spaced uniformly by a distance d as:

$$E(\theta) = \sum_{n=1}^{N} E_n(\theta)\ \exp\left(jknd\cos\theta\right) x_n\, \rho_n, \tag{2}$$

where k is the wavevector, θ is the angle measured from the array axis, and E_n, x_n, ρ_n are the element pattern, excitation, and fault state (1 if the element is working, and 0 if it has failed) of the n^{th} element, respectively. The expression can easily be generalized for planar arrays or near field measurements.

We first sketch the conventional scheme of fault diagnosis where measurements are taken at different locations in space. Assuming for simplicity that the elements are identical (with pattern E_0), and M measurements are taken at locations: $\{\theta_m\}_{m=1}^{M}$, (2) becomes:

$$\tilde{y} = A\,\rho, \quad A_{mn} = E_0 \exp(jnkd\cos\theta_m)x_n, \tag{3}$$

where $\tilde{y} \in \mathbb{C}^M$, $\rho \in \mathbb{C}^N$ represent the vectors of measurements and sensor fault states, respectively, and $A \in \mathbb{C}^{M\times N}$ is the system sensing matrix. Evidently, the only control over designing the system matrix comes by adjusting the measurement locations, θ_m.

Our key observation is that (2) can also be recast in the following way, with an allowance for using different excitations for each measurement at the fixed observation angle, θ_0, as:

$$\tilde{y} = B\rho, \quad B_{mn} = E_0 \exp(jnkd\cos\theta_0)\, x_{mn}, \tag{4}$$

where x_{mn} is the excitation of the n^{th} element for the m^{th} observation, and $B \in \mathbb{C}^{M\times N}$ is the new system matrix. Since the element excitations have entered the system matrix, one can aim to improve the efficiency of fault diagnosis by optimizing the element excitations; this will be demonstrated shortly. The contrast between the conventional and proposed methods is shown graphically in Figure 1.

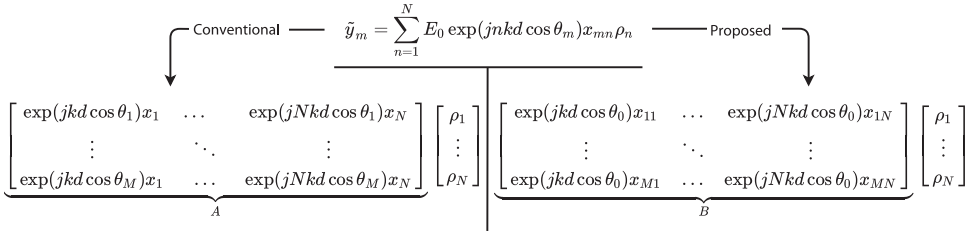

Figure 1. A mathematical counterpart to the schematic in Figure 2, showing the difference between the conventional and proposed method to generate a set of measurements. In the former, measurement locations θ_i are varied, keeping element excitations constant. In the latter, the measurement location is kept constant, while element excitations x_{ij} are varied. Due to the lower mutual coherence obtainable from matrix B, the proposed method gives high success in fault diagnosis. For the sake of illustration, we have set $E_n(\theta) = E_0$, a constant, in (2).

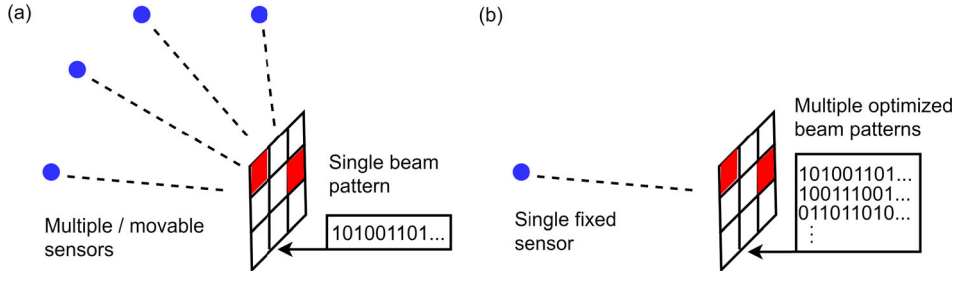

Figure 2. Contrast between (a) conventional, and (b) the proposed method for fault detection. A sample 3×3 phased array is shown by means of a grid, with the filled tiles indicating a faulty element. The filled circles indicate a field measurement sensor, the dashed lines indicate wave propagation between the array and the sensor(s), and a single line of a binary pattern indicates the inputs to the amplitude and phase control of the phased array. For the proposed method, the input signals are optimized in order to minimize the mutual coherence of the sensing matrix. Figure 1 shows a mathematical depiction of the same idea.

To complete the connection with compressive sensing, we refer to the measurements obtained from the 'healthy' array, recorded in $\hat{y} \in \mathbb{C}^M$, and denote the difference in measurements between the healthy and faulty array by $y = \hat{y} - \tilde{y}$. We assume that the number of faults is a small fraction of the total element number, N, and the fault state is binary (i.e. ρ_n is either 0 or 1). As a result, the vector given by $\mathbf{1} - \rho$ is sparse (with $\mathbf{1} \in \mathbb{R}^N$ being a vector of ones). Therefore, the problem that needs to be solved for fault diagnosis becomes:

$$\min_z \|z\|_0, \quad \text{s.t. } \|y - Bz\|_2 < \eta, \tag{5}$$

where $z = \mathbf{1} - \rho$ and η is a small scalar proportional to the variance of measurement noise. We have defined the problem statement for far field measurements with identical elements for ease of illustration. However, we emphasize that our methods are completely general, and demonstrate the generalizations required to deal with heterogeneous arrays and near field measurements in the Appendix.

2.2. Solution philosophy and methodology

As the name 'phased array' suggests, the element excitations have phase and or amplitude control, thus providing a larger canvas to design the sensing matrix than is possible by adjusting receiver positions only.

It is known that the mutual coherence, μ, of a general $M \times N$ fat matrix is lower bounded by the Welch bound, $\sqrt{\frac{N-M}{M(N-1)}} \leq \mu \leq 1$, and that alternating projection algorithms can be used for designing matrices which approach this bound [16,17]. Of great interest is the improvement in performance (e.g. a reduction in the number of measurements) on account of a reduction in μ. Worst case analysis, which tends to be rather pessimistic, says that a signal can be reconstructed from compressive measurements only if it has a sparsity factor (i.e. its 0-norm) up to $O(1 + \frac{1}{\mu})$; on the other hand, when average case performance is sought, the sparsity factor can be up to $O(\frac{1}{\mu^2})$ [15, Thm. 7.3]. Since $\mu < 1$, this means that for a given number of measurements, a greater number of faults can be detected if the sensing matrix is optimized to have lower mutual coherence.

The idea of optimizing the mutual coherence of the sensing matrix and not using a random matrix is one of the key ideas of our work, and a distinguishing feature compared to recent literature [14]. This allows a reduction of the needed number of measurements for a successful fault diagnosis. This reduced number can be an important factor in multiple scenarios, for e.g. : (1) when the forward model used to compute the radiation pattern has a significant computational cost when changing excitation signals (e.g. see reconfigurables reflectarray antennas in [18]), and (2) when the fault diagnosis performed in an onsite way has to minimally affect the operation time of the antenna array. The numerical results in the subsequent Section amply demonstrate the power of our approach.

Often, the nonconvex, combinatorial $\|z\|_0$ function in (5) above is relaxed to $\|z\|_1$, since this is the closest convex function to the ℓ_0 function. Another approach that is considered is the relaxation to the nonconvex function given by $\|z\|_p$ with $0 < p < 1$. Although this nonconvex relaxation does not come with convergence guarantees, it has been empirically found to outperform the ℓ_1 convex relaxation [14,19]. These approaches are summarized in terms of the following unconstrained optimization problem to be solved for fault diagnosis:

$$\min_z \|y - Bz\|_2 + \lambda \|z\|_p, \quad 0 < p \leq 1, \tag{6}$$

where λ is an empirical hyperparameter.

In our work, we assume that the phase and amplitude of the phased array is quantized to 6 bits each to reflect realistic hardware for phase shifters. In implementing related work [14], we generate the amplitude (0 to 1) and phase (0 to 2π) by drawing from the multinomial probability distribution function. In our optimized matrix approach, we initialize with the earlier random matrix, then apply an alternating projection procedure [15, Ch. 2][16], and end by quantizing the amplitude and phase to 6 bits each. The behavior of the mutual coherence values of the matrices used in the results below are shown in Figure 3. It can be seen that even after quantization, the optimized matrices closely approach the Welch bound (attained by Grassmanian matrices [15]).

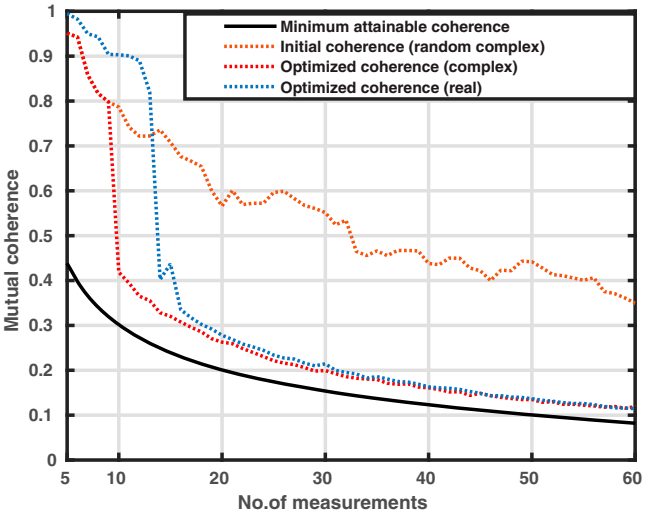

Figure 3. Mutual coherence values for $M \times 100$ matrices for random, optimized, and real sensing matrices. The amplitude and phase of every matrix element has been quantized to 6 bits each in the case of complex measurements, whereas this quantization is to 6 bits amplitude and 1 bit phase (i.e. a $\pm$ sign), in the case of real measurements.

2.3. Approach for real measurements

We now discuss the case of the new type of 'real' measurements proposed in this Article. The essential idea can be distilled by inspecting (2), and noting that if the element patterns, E_n, and excitations, x_{mn}, are real valued and measured at $\theta = \frac{\pi}{2}$ using our proposed approach, then the measured field, $\tilde{y}_m$, given by:

$$\tilde{y}_m = \sum_{n=1}^{N} E_n x_{mn}\, \rho_n, \quad 1 \leq m \leq M, \tag{7}$$

is also real valued. Thus, no information of the fault state is lost by using a sensor capable of only real-valued measurements. In a practical scenario, the radiation pattern of an antenna element need not be real valued. However, using an extension of our method detailed in Appendix 1, it is possible to restrict the field at a measurement point to be real valued by appropriately engineering the element excitations.

For the case of optimizing the sensing matrix here, we restrict the phase to only 1 bit (i.e. a phase of 0 or π), and allow 6 bits of amplitude control as before. Again, we emphasize that the restriction of real valued element patterns and $\theta = \frac{\pi}{2}$ are for illustrative purposes only, and we demonstrate the lifting of these simplifications in the Appendix.

2.4. Summary of proposed algorithm

Based on the theory described above, our approach to diagnosing the faults in an antenna array takes the following steps:

(1) Choose M, the number of measurements to be taken, and initialize the $M \times N$ system matrix, B, as defined in (4) with random excitations, $\{x_{mn}\}$.
(2) Optimize the excitations, $\{x_{mn}\}$, to minimize the mutual coherence of the system matrix B, and quantize the excitations to the available resolution of bits in amplitude and phase.
(3) After subtracting the healthy array measurements from the obtained measurements, solve the optimization problem in (6) to obtain the sensor fault state vector, ρ.

The system matrix obtained in Step (2) above differs depending on whether the measurements are complex or real, as has already been described previously. In the next Section, we provide details of the algorithms used and the results obtained. In particular, we quantify the number of measurements required to guarantee successful fault diagnosis as per a 'rate of successful recovery' defined subsequently.

3. Results & analysis

Algorithms: In this Article, we present the solution to the fault diagnosis problem by three strategies:

(i) A solution to the original problem in (5) by means of a greedy pursuit algorithm, the Compressive Sampling Matching Pursuit (CoSaMP) [20],

(ii) and (iii) Solutions to the relaxed convex and nonconvex problem in (6) with $p = 1$, and $0 < p < 1$, respectively, by means of an iteratively reweighted ℓ_1 (IRL1) minimization algorithm [21] implemented via the alternating direction method of multipliers (ADMM) [22].

Error metrics: We report fault diagnosis success as a *rate of successful recovery* (RSR), which is a metric computed on the recovered solution vector, ρ. RSR-k is the number of measurements such that k% of trials give a perfect reconstruction of the fault state of the array (noting that our definition is more explicit than [14], where RSR is defined in terms of the mean squared error (MSE) being < -30 dB). Further, we implement a thresholding function on the reconstructed vector prior to computing the RSR (i.e. if $\rho_n < 0.5$, set $\rho_n = 0$, else set $\rho_n = 1$). In our simulations, we consider 200 Monte Carlo trials for every result shown.

Implementation details: Note that CoSaMP requires a priori information of the expected sparsity of the solution vector. Since this information is typically not known, we run the algorithm with various guesses (1 to 20) for the solution sparsity. Of those, we pick the sparsity corresponding to the smallest residual error.

In the ℓ_p norm relaxation algorithm, we determine the λ hyperparameter of (6) empirically using a grid search. A study of this search is shown in Figure 4 where the value of λ is varied logarithmically. We find that $\lambda = 0.1$ worked the best for optimized matrices, while $\lambda = 0.01$ was optimal for random matrices. The termination criteria used in CoSaMP and IRL1 is a limit on the total number of iterations (500 in our case). For every result, we perform 200 Monte Carlo iterations; simulations were performed on an Intel Core i7-8700 CPU 3.20 GHz $\times$ 12 processor and took 45–50 seconds on average for IRL1 and 3-4 minutes for CoSaMP.

Comparative results for varying fault numbers: We consider a 100-element linear array consisting of ideal isotropic radiators with measurements at $\theta = \frac{\pi}{2}$ in the far field (noise corrupted with a signal to noise ratio (SNR) of 10 dB). The centerpiece of our results is

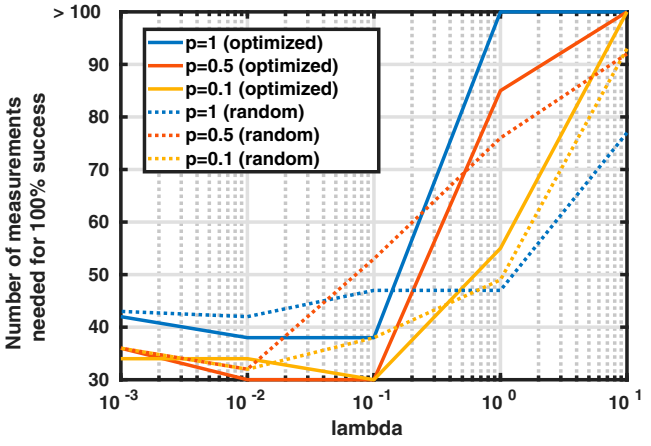

Figure 4. Performance of IRL1 on a 100 element linear array for different values of the hyperparameter, λ for the case of (complex) random and optimized sensing matrices. The number of faults and SNR are fixed at 10 and 20 dB, respectively.

Table 1. Measurements required as a function of number of fault: Number of measurements required to achieve RSR-100 (top rows) and RSR-90 (bottom rows) as a function of fault number, *s*, for a 100-element array and 10 dB SNR. Boldface entries denote the best results for that particular value of *s* and RSR-*k*. R,O,E refer to random, optimized, and real matrices, respectively. The symbol ◇ refers to cases where the number of measurements exceed the number of elements (N) and compressive sensing is no longer meaningful.

	IRL1 $p = 1$			IRL1 $p = 0.5$			IRL1 $p = 0.1$			CoSaMP		
s	R	O	E	R	O	E	R	O	E	R	O	E
Number of measurements for RSR-100 ↓												
1	13	11	15	10	10	15	**9**	**9**	14	34	15	27
5	58	39	49	61	36	56	59	**25**	64	79	48	63
10	◇	69	79	◇	**61**	80	◇	63	91	99	70	84
15	◇	80	99	◇	**71**	94	◇	79	98	◇	80	99
Number of measurements for RSR-90 ↓												
1	9	9	10	**6**	**6**	10	**6**	**6**	10	13	10	14
5	34	30	36	28	20	34	30	**19**	40	47	34	50
10	◇	53	59	◇	43	63	◇	**38**	68	77	58	66
15	◇	67	77	◇	**61**	79	◇	65	86	97	67	82

Table 1, where varying numbers of faults are diagnosed by a variety of methods, including our optimized matrix approach, the random matrix approach from [14], as well as the real-measurements case.

Comparative results for varying SNR: Next, in Table 2 we consider the same array as above, except that we fix the number of faults to 10, and vary the SNR on the measurements.

Comparative results for varying array size: Finally, in Table 3 we consider the performance of various algorithms against varying array sizes, keeping the number of faults and SNR fixed at 10 and 10 dB, respectively.

Analysis: We now analyze the results that we have obtained, drawing out the salient features of our work.

Table 2. Measurements required as a function of SNR: Number of measurements required to achieve RSR-100 (top rows) and RSR-90 (bottom rows) as a function of SNR, for an 100-element array and a fixed number of faults, $s = 10$. Boldface entries denote the best results for that particular value of SNR and RSR-*k*. Other symbols are as in Table 1.

	IRL1 $p = 1$			IRL1 $p = 0.5$			IRL1 $p = 0.1$			CoSaMP		
SNR	R	O	E	R	O	E	R	O	E	R	O	E
Number of measurements for RSR-100 ↓												
10	◇	65	75	◇	**55**	82	◇	65	85	100	64	85
20	40	38	47	31	**29**	43	33	30	45	34	30	42
30	38	35	44	31	**28**	41	32	30	44	29	30	40
Number of measurements for RSR-90 ↓												
10	◇	53	62	◇	39	61	◇	**37**	69	70	51	67
20	36	32	40	28	**24**	36	28	26	39	27	26	35
30	33	31	37	26	**24**	35	29	25	40	26	26	34

Table 3. Number of measurements required to achieve RSR-100 (top rows) and RSR-90 (bottom rows) as a function of array size, *N*, for a fixed number of faults, $s = 10$, and 10 dB SNR. Boldface entries denote the best results for that particular value of *N* and RSR-*k*. Other symbols are as in Table 1.

	IRL1 $p = 1$			IRL1 $p = 0.5$			IRL1 $p = 0.1$			CoSaMP		
N	R	O	E	R	O	E	R	O	E	R	O	E
Number of measurements for RSR-100 ↓												
50	◇	42	◇	◇	43	◇	◇	**40**	◇	◇	50	◇
70	◇	51	◇	◇	**46**	68	◇	57	69	◇	52	◇
90	◇	65	69	◇	**56**	74	◇	61	84	85	57	78
Number of measurements for RSR-90 ↓												
50	◇	36	41	◇	**31**	41	◇	33	44	◇	39	48
70	◇	43	52	◇	**33**	53	◇	35	51	63	44	58
90	◇	51	57	◇	39	59	◇	**37**	66	63	50	62

(1) The results in all the Tables strongly suggest that regardless of the algorithm used, the optimized matrix approach *always* outperforms the random matrix approach under varying number of faults, noise levels, as well as different array sizes. The difference between the optimized and random matrix approaches becomes clearer as the number of faults increases. This is to be expected from the study of the mutual coherence (see Figure 3), where an improvement as compared to the random matrix case is seen only after the number of measurements exceeds 9 (for an arrary of 100 elements).

(2) We emphasize that our approach is particularly robust under high noise conditions; in particular, as the (10 dB SNR) results in Table 1 show, in most cases the random matrix approach fails (marked by a diamond symbol indicative of $> N$ measurements, at which point a brute force approach of testing each element individually is better). In general it is seen that the optimized matrix approach takes 1-2 times *fewer* measurements than the random sensing matrix case.

(3) A remarkable observation from all the results is that the number of measurements required for the case of real measurements is comparable with that from the random sensing matrix case with complex measurements. In fact, in several instances the former succeeds, while the latter fails.

(4) Among the methods considered in this Article, the IRL1 algorithm with $p = 0.5$ delivers the best results, though the results with $p = 0.1$ are only slightly worse in comparison. The results of the CoSaMP algorithm are also competitive.

4. Conclusion

In summary, we have presented a new framework in which fault diagnosis can be performed on phased arrays without taking recourse to moving detectors in space. Our approach optimizes the element excitations and leverages ideas from compressive sensing to perform this diagnosis, giving us two distinct advantages with respect to the most advanced state-of-the-art: the fault diagnosis can be done with (a) fewer measurements, and (b) in the presence of real measurements. We show the superior performance of our methods through extensive numerical simulations; in particular, we show how our methods are robust in the presence of noise, delivering results when other methods fail. Finally, our methods can easily be generalized to near field measurements of heterogeneous arrays.

A practical way in which the proposed method can be used to diagnose faults in newer antenna systems with modulated waveforms (e.g. 5G communication systems) is to introduce specific time frames during which the array radiates narrow band signals for purely diagnostic purposes. Since only a small number of electronic signals corresponding to well-chosen element excitations need to be generated, no significant downtime in regular device operation is expected. Also, potential extensions of our algorithm to use modulated signals as diagnostic signals instead of narrow band signals is of interest and it will be investigated as future work. The model used in our Article does not consider mutual coupling effects, which we consider beyond the scope of our current work. Taking into account mutual coupling among antenna elements could require more computationally expensive electromagnetic solvers and increase the CPU time needed by the algorithm to identify faults. Another aspect to be investigated as future work is how the mutual coherence of the sensing matrix could be affected by taking into account mutual coupling effects.

Acknowledgements

The authors acknowledge useful discussions on array fault diagnosis with Rajat Vadiraj Dwaraknath, IIT Madras.

Disclosure statement

No potential conflict of interest was reported by the author(s).

Notes on contributors

K. P. Prajosh is currently pursuing the Ph.D. degree at the Indian Institute of Technology Madras, India. He received an M.Tech degree in RF & Microwave Engineering from the Indian Institute of Space Science and Technology, Thiruvananthapuram, India, and B.Tech degree in Electronics & Communication engineering from the University of Calicut, India. His research interests include inverse problems in electromagnetics and compressive sensing.

Uday K. Khankhoje is an Assistant Professor of Electrical Engineering at the Indian Institute of Technology Madras, India. He received a B.Tech. degree from the Indian Institute of Technology Bombay, India, in 2005, an M.S. and Ph.D. degrees from the California Institute of Technology, Pasadena, USA,

in 2010, all in Electrical Engineering. He was a Caltech Postdoctoral Scholar at the Jet Propulsion Laboratory (NASA/Caltech) from 2011-2012, a Postdoctoral Research Associate in the Department of Electrical Engineering at the University of Southern California, Los Angeles, USA, from 2012–2013, and an Assistant Professor of Electrical Engineering at the Indian Institute of Technology Delhi, India from 2013-16. His research interests lie in the area of computational electromagnetics and its applications to remote sensing and inverse imaging.

Francesco Ferranti is an Associate Professor with the Microwave Department, Institut Mines-Télécom (IMT) Atlantique, Brest, France. His research interests include data-driven and model-driven modeling techniques, sampling techniques, design space exploration, uncertainty quantification, optimization, applied electromagnetics, behavioral modeling, microwave design and characterization.

ORCID

K. P. Prajosh http://orcid.org/0000-0002-2160-2655
Uday K. Khankhoje http://orcid.org/0000-0002-9629-3922
Francesco Ferranti http://orcid.org/0000-0003-1060-3713

References

[1] Hansen RC. Phased array antennas. Vol. 213. Hoboken (NJ): John Wiley & Sons; 2009.
[2] Hong W, Baek KH, Ko S. Millimeter-wave 5g antennas for smartphones: overview and experimental demonstration. IEEE Transactions on Antennas Propagation. 2017 Dec;65(12):6250–6261.
[3] Menzel W, Moebius A. Antenna concepts radar sensors. Proceedings of the IEEE. 2012 July;100(7):2372–2379.
[4] Castorina G, Di Donato L, Morabito AF, et al. Analysis and design of a concrete embedded antenna for wireless monitoring applications [antenna applications corner]. IEEE Transactions on Antenna and Propagation M. 2016;58(6):76–93.
[5] Donoho DL. Compressed sensing. IEEE Transaction on Information Theory. 2006 Apr;52(4):1289–1306.
[6] Migliore MD. A compressed sensing approach for array diagnosis from a small set of near-field measurements. IEEE Transactions on Antennas Propagation. 2011 June;59(6):2127–2133.
[7] Migliore MD. Array diagnosis from far-field data using the theory of random partial fourier matrices. IEEE Antennas and Wireless Propagation Letters. 2013;12:745–748.
[8] Oliveri G, Rocca P, Massa A. Reliable diagnosis of large linear arrays'a bayesian compressive sensing approach. IEEE Transactions on Antennas Propagation. 2012 Oct;60(10):4627–4636.
[9] Morabito A, Palmeri R, Isernia T. A compressive-sensing-inspired procedure for array antenna diagnostics by a small number of phaseless measurements. IEEE Transactions on Antennas Propagation. 2016 July;64(7):3260–3265.
[10] Candes EJ. The restricted isometry property and its implications for compressed sensing. Comptes Rendus Mathematique. 2008;346(9–10):589–592.
[11] Candes E, Romberg J. Sparsity and incoherence in compressive sampling. Inverse Probl. 2007;23(3):969.
[12] Obermeier R, Martinez-Lorenzo JA. Sensing matrix design via mutual coherence minimization for electromagnetic compressive imaging applications. IEEE Trans Comput Imag. 2017 June;3(2):217–229.
[13] Eltayeb ME, Al-Naffouri TY, Heath RW. Compressive sensing for millimeter wave antenna array diagnosis. IEEE Trans Commun. 2018 June;66(6):2708–2721.
[14] Xiong C, Xiao G, Hou Y, et al. A compressed sensing-based element failure diagnosis method for phased array antenna during beam steering. IEEE Antennas Wirel Propag Lett. 2019 Sept;18(9):1756–1760.
[15] Elad M. Sparse and redundant representations: from theory to applications in signal and image processing. 1st ed. New York: Springer-Verlag; 2010.

[16] Dhillon I, Heath Jr R, Strohmer T, et al. Designing structured tight frames via alternating projection. IEEE Transactions on Information Theory. 2005 Jan;51(1):188–209.
[17] Hong T, Bai H, Li S, et al. An efficient algorithm for designing projection matrix in compressive sensing based on alternating optimization. Signal Processing. 2016;125:9–20.
[18] Yann C, Loison R, Gillard R, et al. A new approach combining surrounded-element and compression methods for analyzing reconfigurable reflectarray antennas. IEEE Transactions on Antennas Propagation. 2012 July;60(7):3215–3221.
[19] Ince T, Ögücü G. Array failure diagnosis using nonconvex compressed sensing. IEEE Antennas Wirel Propag Lett. 2015;15:992–995.
[20] Needell D, Tropp JA. Cosamp: iterative signal recovery from incomplete and inaccurate samples. Appl Comput Harmon Anal. 2009;26(3):301–321.
[21] Foucart S, Lai MJ. Sparsest solutions of underdetermined linear systems via ℓ_q-minimization for $0 < q \leq 1$. Appl Comput Harmon Anal. 2009;26(3):395–407.
[22] Boyd S, Parikh N, Chu E, et al. Distributed optimization and statistical learning via the alternating direction method of multipliers. Foundations and Trends® in Machine Learning. 2011;3(1):1–122.

A. Appendix 1. Heterogeneous arrays, near field measurements

We consider the case where the array elements are heterogeneous, and the (possibly near-field) measurements may be away from the normal direction (i.e. $\theta \neq \frac{\pi}{2}$). In this most general case (still ignoring mutual coupling, though), (2) gets generalized to:

$$E(r,\theta) = \sum_{n=1}^{N} E_n(r_n,\theta_n)\, x_n\, \rho_n. \tag{A1}$$

For e.g. if a particular element were a Hertz dipole at the origin, and we were measuring the θ-component of the field, $E_\theta(r,\theta)$, we would have $E_n(r_n,\theta_n) = -jZ_0 I e^{-jkr_n}/(4\pi k r_n^3)\sin\theta_n$, where I is the dipole length and Z_0 is free space impedance.

We define a matrix of excitations, $X \in \mathbb{C}^{M\times N}$ s.t. $X_{mn} = x_{mn}$, a vector $t \in \mathbb{C}^N$ s.t. $t_n = E_n(r_n,\theta_n)\rho_n$, a vector $\tilde{t} \in \mathbb{C}^N$ s.t. $\tilde{t}_n = E_n(r_n,\theta_n)$, and a diagonal matrix $W \in \mathbb{C}^{N\times N}$ s.t. $W_{nn} = 1/E_n(r_n,\theta_n)$. Then the fault diagnosis optimization problem is similar to the earlier (5) with a re-definition of z to guarantee its sparsity, as below:

$$\min_z \|Wz\|_0, \text{ s.t. } \|y - Xz\|_2 < \eta, \text{where } z = \tilde{t} - t. \tag{A2}$$

With the identical reformulation of z, the nonconvex relaxation described by (6) can be used in this general setting. Thus, as desired, the system matrix X can be completely optimized for fault diagnosis even in this general setting. The proposed method is also applicable for fault diagnosis in a planar array.

Real measurement scenario: In this case, the principle is to use the phase of the excitation, x_n, to cancel the phase of the accompanying $E_n(r_n,\theta_n)$ term of (A1). While the phase is restricted in this manner (up to a sign), we are free to adjust the amplitude of the excitations to optimize the sensing matrix. As a result, the measurement, $E(r,\theta)$, is real valued. This approach depends on there being sufficient bits available for phase control to approximate the negative of the phase of $E_n(r_n,\theta_n)$.